JOC Article

Synthesis and Self-Assembly of Glycal-Based Bolaforms

Joseph J. Bozell,*[,†] Nathan C. Tice,[†] Nibedita Sanyal,[†] David Thompson,[‡] Jong-Mok Kim,[‡] and Sébastien Vidal[§]

Biomass Chemistry Laboratories-Forest Products Center, University of Tennessee, Knoxville, Tennessee 37996, Department of Chemistry, Purdue University, West Lafayette, Indiana 47907, and Institut de Chimie et Biochimie Moléculaires et Supramoléculaires, UMR 5246, CNRS, INSA Lyon, CPE-Lyon, Université Claude Bernard Lyon 1, Lyon, France

jbozell@utk.edu

Received June 27, 2008

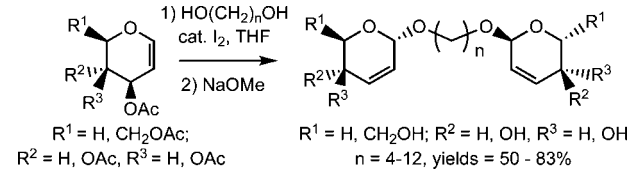

Glycal-based bolaforms serve as synthetically flexible components of molecular self-assembly. The compounds are prepared in good yield by a Ferrier reaction between triacetylglucal or -galactal or diacetylxylal and a long chain α,ω-diol, followed by deacetylation under Zemplén conditions. The reactions are stereoselective and preferentially afford the α-diastereomer. The bolaforms undergo self-assembly in water or water/dioxane solution to give a variety of nanostructures. In solution, bolaforms with C_8 or C_{10} chains between glucal headgroups form nanoscale vesicles. In contrast, bolaforms with C_{12} chains exhibit lower solubility and a dynamic self-assembly, forming several different nanoscale structures. However, the solid-state structures of C_{12} bolaform isomers adopt shapes very similar to those of bolaforms possessing more extensive hydrogen-bonding networks, indicating that multiple hydrogen bonds in solution are important to formation of stable, discrete nanostructures but that only a few key intermolecular interactions between bolaform headgroups are necessary to determine the structure in the solid state. The diversity and differentiation of the functional groups present in glycal-based bolaforms suggest that they could be useful probes of the various noncovalent forces controlling the structure of new nanomaterials.

Introduction

Molecular self-assembly provides access to a wide range of nanoscale materials in chemical and biological processes and offers a way to build complex structures in a controlled manner from smaller particles.[1] Within the context of organic synthesis, interest in self-assembling systems represents an important transition from stepwise formation of covalent bonds to processes that create stable, noncovalent networks between individual molecules.[2] Thermodynamic models based on molecular volumes have been used to calculate packing parameters able to describe the observed shapes of various polymolecular assemblies.[3] However, predicting the topography of a nanoscale material based on individual structural and electronic features of its molecular components is not as well understood as the synthetic processes used to make its separate parts. The noncovalent forces controlling self-assembly must often balance hydrogen and van der Waals bonding, $\pi-\pi$ interactions, and molecular hydrophobicity/hydrophilicity. New, self-assembling molecules with sufficient synthetic flexibility to allow straightforward, systematic evaluation of these various forces would be useful for developing shape/structure correlations.

Bolaforms are self-assembling molecules characterized by a long hydrophobic spacer connecting two hydrophilic headgroups.[4] Depending on their structure, bolaforms undergo self-assembly into nanoscale micelles, monolayer membranes, or vesicles. A number of reports describe naturally occurring

[†] University of Tennessee.
[‡] Purdue University.
[§] Université Claude Bernard Lyon 1.

(1) (a) Zhang, S. *Nat. Biotechnol.* **2003**, *21*, 1171. (b) Whitesides, G. M.; Grzybowski, B. *Science* **2002**, *295*, 2418.

(2) (a) Leininger, S.; Olenyuk, B.; Stang, P. J. *Chem. Rev.* **2000**, *100*, 853. (b) Philp, D.; Stoddart, J. F. *Angew. Chem., Int. Ed. Engl.* **1996**, *35*, 1155. (c) Whitesides, G. M.; Mathias, J. P.; Seto, C. T. *Science* **1991**, *254*, 1312. (d) Hosseini, M. W. *Acc. Chem. Res.* **2005**, *38*, 313.

(3) (a) Tanford, C. *J. Phys. Chem.* **1972**, *76*, 3020. (b) Israelachvili, J. N.; Mitchell, D. J.; Ninham, B. W. *J. Chem. Soc., Faraday Trans.* **1976**, *72*, 1525. (c) Yan, Y.; Xiong, W.; Li, X.; Lu, T.; Huang, J.; Li, Z.; Fu, H. *J. Phys. Chem. B* **2007**, *111*, 2225.

(4) Fuhrhop, J.-H.; Wang, T. *Chem. Rev.* **2004**, *104*, 2901.

10.1021/jo801341g CCC: $40.75
Published on Web 10/17/2008

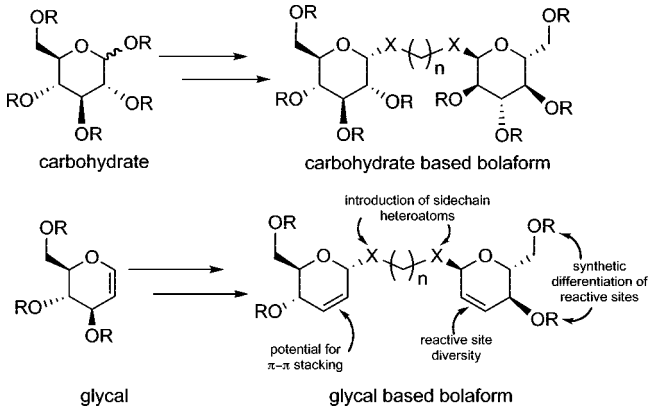

FIGURE 1. Comparison of carbohydrate- and glycal-based bolaforms.

carbohydrates as bolaform headgroups[5] and the hydrogen-bonding networks present in both nanoscale assemblies and the solid state resulting from headgroup stereochemistry.[6] Relatively subtle changes in headgroup structure have been found to significantly alter the structure of the self-assembled array, suggesting that carbohydrate-based bolaforms could serve as useful probes of shape/structure correlations.[7] However, the utility of carbohydrate headgroups in this role is limited by multistep syntheses,[8] low yields,[9] or a lack of simple approaches for regiospecific modification of the sugar's secondary C-2, C-3, or C-4 hydroxyl groups. As part of our program examining renewable building blocks and their derivatives as sources of new nanostructural materials,[10] we are investigating glycals (1,2-unsaturated glycopyranosides) as alternative bolaform headgroups because they are subject to a much wider range of synthetic transformations, exhibit clear differentiation of each reactive site, and offer the potential of enhanced self-assembly via $\pi-\pi$ stacking of the double bond (Figure 1). We wish to report a simple Ferrier synthesis of several glycal-based bolaforms and our initial investigation of how the structural differences between glycal-based bolaforms and those derived from conventional carbohydrates are manifested during self-assembly.

Results and Discussion

Bolaform Synthesis. Our synthetic approach and results are summarized in Scheme 1. Glycal-based bolaforms are synthesized using an iodine catalyzed Ferrier reaction.[11] Treatment of the glycal with a long-chain α,ω-diol in the presence of 3−5% I_2 in THF gives the corresponding bolaform as the acetate. Deacetylation under Zemplén conditions (5% NaOMe in MeOH) affords the hydroxylated bolaform. The process is general, and gives fair to excellent yields of product from triacetylglucal **1a** (compounds **3a**−**d**) and -galactal **1b**[12] (compound **3e**) and diacetylxylal **1c**[13] (compound **3f**) via the intermediate acetates **2a**−**f**.

SCHEME 1. Synthesis of Glycal-Based Bolaforms

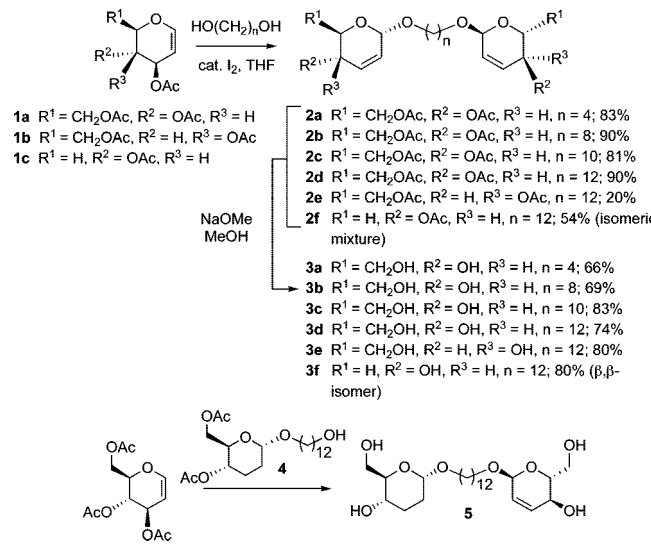

The length of the linking chain has little effect on the reaction as high yields are observed using diols with chains containing 4−12 carbon atoms. The synthesis can also be carried out in a stepwise manner to give unsymmetrical bolaforms. Ferrier reaction of triacetylglucal with the mono-THP ether of 1,12-dodecanediol followed by hydrogenation over 5% Pd/C gives alcohol **4**. Ferrier reaction with a second equivalent of triacetylglucal followed by deacetylation leads to unsymmetrical bolaform **5** (76 and 50% yield for the two reactions, respectively).

Consistent with standard Ferrier reactions, triacetylglucal undergoes a thermodynamically controlled addition of diol to give a roughly 70:30 (by NMR) mixture of α,α to α,β adducts.[14,15] Use of other Lewis acids such as BF_3 etherate, SnCl4,[16] or $NbCl_5$[17] did not improve the stereochemical ratio.

(5) (a) Garelli-Calvet, R.; Brisset, F.; Rico, I.; Lattes, A. *Synth. Commun.* **1993**, *23*, 35. (b) Pestman, J. M.; Terpstra, K. R.; Stuart, M. C. A.; van Doren, H. A.; Brisson, A.; Kellogg, R. M.; Engberts, J. B. F. N. *Langmuir* **1997**, *13*, 6857. (c) Prata, C.; Mora, N.; Polidori, A.; Lacombe, J.-M.; Pucci, B. *Carbohydr. Res.* **1999**, *321*, 15. (d) Lafont, D.; Boullanger, P.; Chevalier, Y. *J. Carbohydr. Chem.* **1995**, *14*, 533.

(6) (a) Masuda, M.; Hanada, T.; Yase, K.; Shimizu, T. *Macromolecules* **1998**, *31*, 9403. (b) Masuda, M.; Shimizu, T. *Carbohydr. Res.* **1997**, *302*, 139.

(7) Masuda, M.; Shimizu, T. *Carbohydr. Res.* **2000**, *326*, 56.

(8) (a) Bertho, J. N.; Coue, A.; Ewing, D. F.; Goodby, J. W.; Letellier, P.; Mackenzie, G.; Plusquellec, D. *Carbohydr. Res.* **1997**, 300–341. (b) Denoyelle, S.; Polidori, A.; Brunelle, M.; Vuillaume, P. Y.; Laurent, S.; El Azhary, Y.; Pucci, B. *New J. Chem.* **2006**, *30*, 629. (c) Abraham, S.; Paul, S.; Narayan, G.; Prasad, S. K.; Rao, D. S. S.; Jayaraman, N.; Das, S. *Adv. Funct. Mater.* **2005**, *15*, 1579. (d) Shimizu, T.; Masuda, M. *J. Am. Chem. Soc.* **1997**, *119*, 2812. (e) Goueth, P.; Ramiz, A.; Ronco, G.; Mackenzie, G.; Villa, P. *Carbohydr. Res.* **1995**, *266*, 171.

(9) Gerber, S.; Garamus, V. M.; Milkereit, G.; Vill, V. *Langmuir* **2005**, *21*, 6707.

(10) (a) Bozell, J. J. *ACS Symp. Ser.* **2006**, *921*, 1. (b) Bozell, J. J.; Hoberg, J. O.; Claffey, D.; Hames, B. R.; Dimmel, D. R. In *Green Chemistry: Frontiers in Benign Chemical Synthesis and Processing*; Anastas, P. T., Williamson, T. C., Eds.; Oxford University Press: Oxford, 1998; Chapter 2.

(11) Koreeda, M.; Houston, T. A.; Shull, B. K.; Klemke, E.; Tuinman, R. J. *Synlett* **1995**, 90.

(12) Prepared by conversion of galactose pentaacetate to the galactosyl bromide and reduction to the galactal with Zn: (a) Litjens, R. E. J. N.; den Heeten, R.; Timmer, M. S. M.; Overkleeft, H. S.; van der Marel, G. A. *Chem.—Eur. J.* **2005**, *11*, 1010. (b) Bukowski, R.; Morris, L. M.; Woods, R. J.; Weimar, T. *Eur. J. Org. Chem.* **2001**, 2697.

(13) Prepared by conversion of xylose to the tetraacetate, bromination to the xylosyl bromide, and reduction to the xylal with Zn: (a) Bhaskar, P. M.; Loganathan, D. *Tetrahedron Lett.* **1998**, *39*, 2215. (b) Mechaly, A.; Belakhov, V.; Shoham, Y.; Baasov, T. *Carbohydr. Res.* **1997**, *304*, 111. (c) Somsak, L.; Nemeth, I. *J. Carbohydr. Chem.* **1993**, *12*, 679.

(14) Ferrier, R. J.; Zubkov, O. A. *Org. React.* **2003**, 569.

(15) Stereochemical assignments are consistent with reported spectra: (a) Achmatowicz, O.; Bukowski, P.; Szechner, B.; Zwierzchowska, Z.; Zamojski, A. *Tetrahedron* **1971**, *27*, 1973. (b) Liu, Z. J.; Zhou, M.; Min, J. M.; Zhang, L. H. *Tetrahedron: Asymmetry* **1999**, *10*, 2119. (c) Ponticelli, F.; Trendafilova, A.; Valoti, M.; Saponara, S.; Sgaragli, G. *Carbohydr. Res.* **2001**, *330*, 459. (d) Fava, C.; Galeazzi, R.; Mobbili, G.; Orena, M. *Tetrahedron: Asymmetry* **2001**, *12*, 2731. (e) de Freitas Filho, J. R.; Srivastava, R. M.; da Silva, W. J. P.; Cottier, L.; Sinou, D. *Carbohydr. Res.* **2003**, *338*, 673.

(16) Grynkiewicz, G.; Priebe, W.; Zamojski, A. *Carbohydr. Res.* **1979**, *68*, 33.

(17) De Oliveria, R. N.; de Melo, A. C. N.; Srivastava, R. M.; Sinou, D. *Heterocycles* **2006**, *68*, 2607.

TABLE 1. Effect of Lewis Acid Catalyst and Solvent on Ferrier Reaction Stereoselectivity

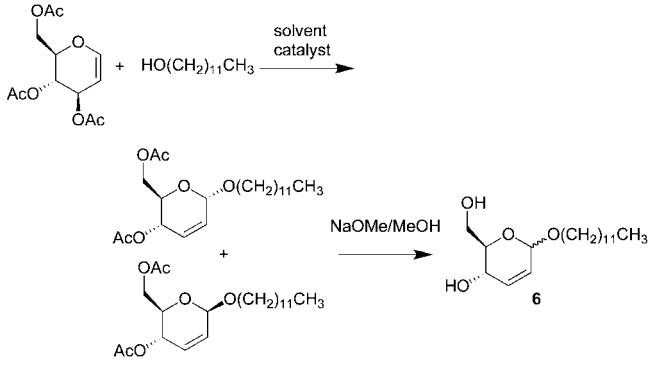

catalyst	solvent	isolated yield of **6** (%)	α/β
I_2	THF	82	12:1
I_2	CH_2Cl_2	86	18:1
I_2	MeCN	80	12:1
$TiCl_4$	THF	71	3:1
$TiCl_4$	CH_2Cl_2	46	3:1
$TiCl_4$	MeCN	*a*	
$TiCl_4$	Et_2O	*a*	
BF_3 etherate	CH_2Cl_2	*a*	
BF_3 etherate	MeCN	*a*	

[a] A mixture of several products resulted from the Ferrier reaction prior to Zémplen deacetylation.

The glycal stereochemistry and structure have a strong influence on the diastereomeric ratio at the anomeric carbon. Triacetylgalactal undergoes a stereospecific (albeit low yield) addition of diol to afford only the α,α product due to the higher level of steric crowding on the β-face, and the influence of the axial acetoxy group at C-4.[18] In contrast, conversion of diacetylxylal to bolaform **3f** exhibits no stereocontrol at the anomeric center, as it lacks both the electronic influence of an axial C-4 acetoxy group and the steric influence of the CH_2OAc group at C-5. Stereochemical assignment of the diacetylxylal derivatives was carried out by comparison of the NMR spectra with those of Ferrier adducts from the literature and verified by X-ray diffraction.

We examined the effect of different reaction conditions on the stereoselectivity of addition using triacetylglucal and 1-dodecanol to isolate reaction at a single anomeric site, leading to amphiphile **6** (Table 1).

Catalytic I_2 as the Lewis acid afforded the highest yield and stereoselectivity in each of the three solvents examined. Using the stronger Lewis acid $TiCl_4$ resulted in lower yields of **6** and poorer stereoselectivity in THF or CH_2Cl_2. $TiCl_4$ led to a complex mixture of products from the Ferrier reaction when used in Et_2O or MeCN. BF_3 etherate, in catalytic or excess amounts, behaved similarly, giving the initial Ferrier adduct in <10% yield when used in CH_2Cl_2 or MeCN. CH_2Cl_2 favors the thermodynamic isomer somewhat more strongly than THF or MeCN, similar to the solvent effect reported for the cyanation of triacetylglucal with TMSCN under Ferrier conditions.[19] When cyanation is carried out in $MeNO_2$ using BF_3 etherate as the Lewis acid, a 57/42 ratio of α and β isomers is observed. However, changing the solvent to CH_2Cl_2 produces the thermodynamic α isomer as the only product in 79% yield. The reasons for this improvement remain unclear, as the anomeric configuration of a Ferrier addition product is under the influence of a wide range of factors.[14] Although higher stereoselectivities were observed in our model system, application of these conditions to bolaform synthesis did not significantly increase stereoselectivity.

Bolaform Self-Assembly. Carbohydrate-based bolaforms and related systems form noncovalently bound nanoscale polymers linked through an extensive hydrogen-bonding network established between the carbohydrate headgroups during self-assembly.[20] The strong influence of this network is demonstrated in certain cases by deformation of the hydrocarbon chain from a normal *trans*-zigzag conformation to accommodate the most stable hydrogen-bonding arrangement present at the headgroup.[7] Although we expected the formation of similar networks during self-assembly of our glycal systems, replacing a carbohydrate with a glycal (Figure 1) results in a marked reduction of the number of hydrogen bonding opportunities and lowers the polarity of the headgroup.

These changes increase the bolaform's sensitivity to other intermolecular forces, such as van der Waals interactions between the hydrophobic chains linking the headgroups. For example, we observe marked solubility differences in water between compounds **3b**−**d** upon increasing the chain length from C_8 to C_{12}. Compound **3b** (C_8) is partially soluble in water at room temperature at concentrations of 20 mg/mL and fully soluble upon gentle warming to give a slightly opaque solution that is stable for weeks at ambient temperature without precipitation. Upon agitation, a solution of **3b** shows mild surfactant properties, developing a soapy foam at the air/water interface. Compound **3c** (C_{10}) dissolves fully in warm water at 20 mg/mL but begins to precipitate upon returning to room temperature. However, **3c** is fully soluble in a 2:1 mixture of water/1,4-dioxane at a concentration of about 15 mg/mL. Compound **3d** (C_{12}) is water soluble at a concentration of 20 mg/mL only at temperatures above 75 °C and rapidly precipitates upon cooling of the solution. Upon heating, the compound dissolves in 1:1 1,4-dioxane/water at a concentration of about 10 mg/mL and remains in solution for a limited time after cooling to room temperature but generally begins precipitation within 24−48 h. Increasing the pH of the solution to approximately 14 with aqueous NaOH or KOH does not improve the solubility of **3d**. Galactal bolaform **3e** (C_{12}) exhibits solubility behavior similar to **3d**.

Two methods were used to disperse bolaforms **3b**−**d** in solution prior to self-assembly. In one method, the bolaform was mixed with an appropriate solvent, heated to complete dissolution, and slowly cooled to room temperature. The second method added 15 min of sonication in an ultrasonic cleaning bath. Two homogeneous solutions of **3b** and **3c**, one freshly prepared, and the other aged for several weeks, were stained with uranyl acetate and imaged using transmission electron microscopy (TEM). Samples of **3b** and **3c** were also subjected to sonication and compared with unsonicated samples.

In aqueous solution at a concentration of 10 mg/mL, **3b** forms isolated vesicles with diameters between 500 nm and 4 μm. The vesicles remained dispersed, with no aggregation observed upon aging (Figure 2A,C). Sonication of either freshly prepared or aged samples had no effect on the observed structures (Figure 2B,D). At higher magnification (Figure 2A), light and very fine

(18) Demchenko, A. V.; Rousson, E.; Boons, G.-J. *Tetrahedron Lett.* **1999**, *40*, 6523.

(19) (a) de las Heras, F. G.; San Felix, A.; Fernández-Resa, P. *Tetrahedron* **1983**, *39*, 1617. (b) Grynkiewicz, G.; BeMiller, J. N. *Carbohydr. Res.* **1982**, *108*, 229.

(20) Shimizu, T.; Masuda, M.; Minamikawa, H. *Chem. Rev.* **2005**, *105*, 1401.

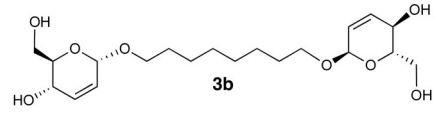

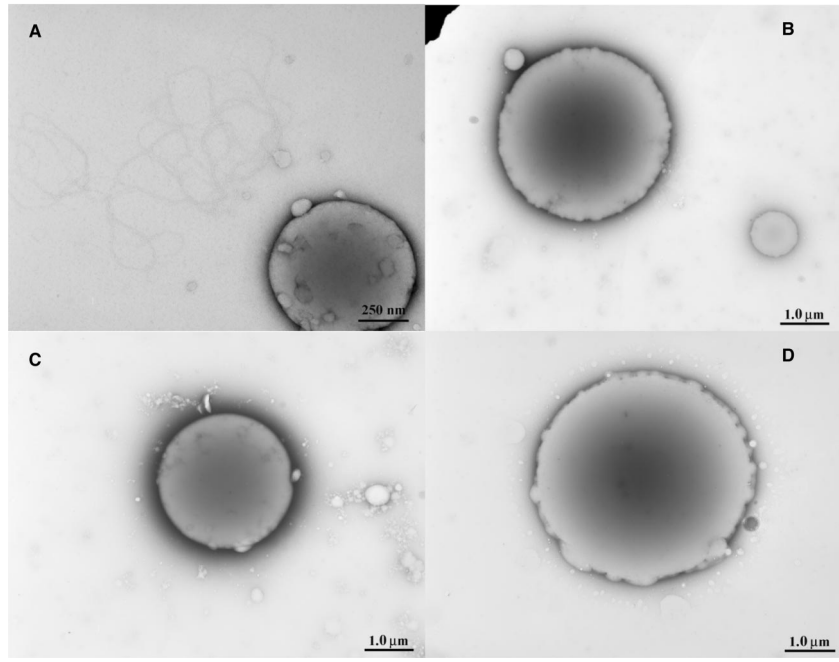

FIGURE 2. TEM images of bolaform **3b** (A, aged, no sonication; B, aged, sonicated; C, fresh, no sonication; D, fresh, sonicated).

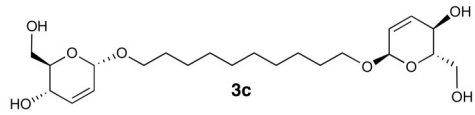

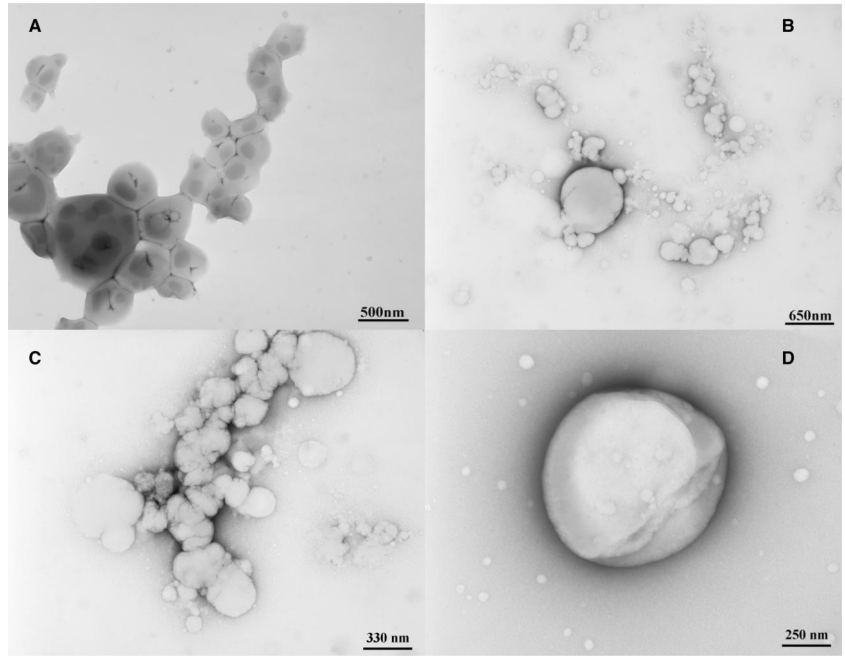

FIGURE 3. TEM images of bolaform **3c** (A, aged, no sonication; B, fresh, sonicated; C, fresh, no sonication; D, aged, sonicated).

threadlike structures were occasionally observed. As the chain length between the headgroups increases, the individual nanostructures associate more strongly with one another, possibly driven by increased influence of the hydrophobic linking chains of the bolaform. In 2:1 water/1,4-dioxane, bolaform **3c** forms groups of vesicles of smaller diameter and somewhat more irregularly shaped than C_8 bolaform **3b** (Figure 3A,C). Aggregation occurs early in the self-assembly process as TEM images of both freshly prepared solutions (Figure 3C) and aged samples show similar clusters of nanostructures. The aggregates

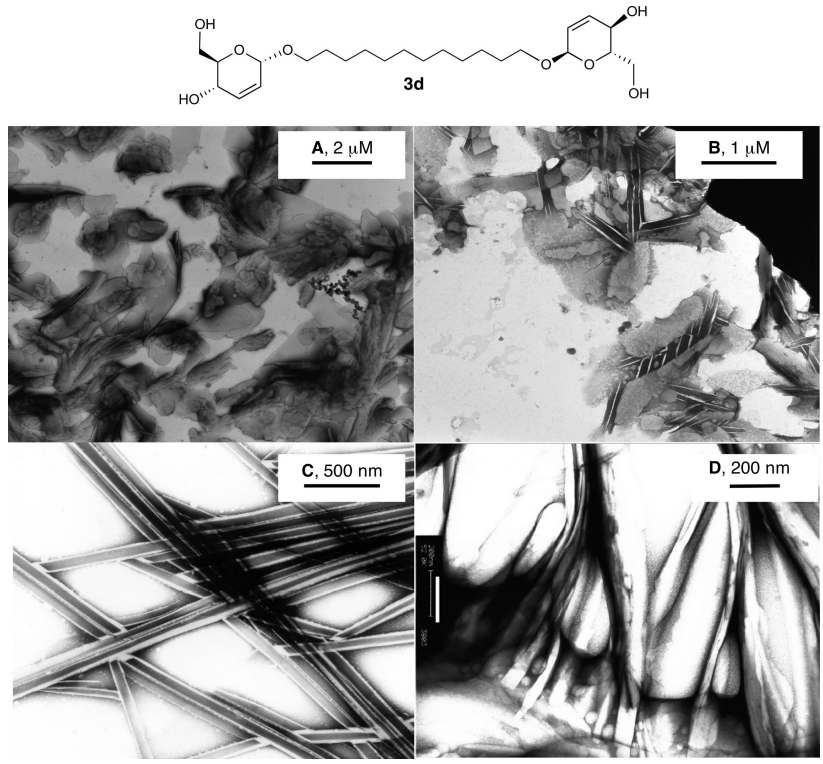

FIGURE 4. TEM images of self-assembled systems from compound **3d**.

can be disrupted by sonication to reduce the size of the clusters (Figure 3B), leading to the appearance of small, isolated vesicles (Figure 3D).

Bolaform **3d** exhibits the greatest diversity of structures upon self-assembly. In 1:1 water/1,4-dioxane, many samples of **3d** show the presence of large plates, sometimes interspersed with tubular structures, suggesting that the limited solubility of **3d** leads to sedimentation or formation of microcrystalline solid during TEM sample preparation (Figure 4A). However, nanoscale tubules with widths of a few hundred nanometers and lengths varying between 500 and several thousand nanometers appear either incorporated with microcrystalline material or as discrete structures (Figure 4A−C). Other samples of **3d** show complex assemblies incorporating both tubes and spherical structures (Figure 4D). Upon standing, aggregation of **3d** ultimately results in formation of fibrous solids as a precipitate. Sonication of samples of **3d** prior to TEM imaging does not lead to isolated structures. Tube formation is reported during self-assembly of carbohydrate-based bolaforms and is shown to be the result of stepwise assembly of individual molecules into vesicles, helical sheets, and ultimately, stable tubes.[21] Further, these structures have been shown to coexist in self-assembling systems.[22] Compound **3d** appears to exhibit similar behavior, and Figure 4D may be capturing intermediates in the process. However, the low solubility of **3d** appears to offer a favorable parallel route to solid formation, overwhelming the ability of **3d** to exist as stable, isolated nanostructures.

X-ray Evaluation of Crystalline Bolaforms. X-ray diffraction of crystalline **3d** and **3e** reveals that hydrogen bonding between headgroups induces considerable order in the solid state. The structures of the major (α,α) and minor (α,β) diastereomers of glucal derivative **3d** and galactal derivative **3e** are shown in Figure 5.[23]

The X-ray structures of bolaforms **3d** and **3e** confirm the stereochemistry of the Ferrier reaction. As anticipated, evaluation of the close contacts in the solid state structure of **3d** and **3e** shows a significant decrease in the number of hydrogen bonds and a modification of the intermolecular network from that reported for similar bolaforms bearing gluco- and galacto-headgroups, respectively. The galacto analogue of **3e** has been reported to have as many as 26 unique hydrogen-bonding interactions in the headgroup network.[7] Close contact analysis of compounds **3d** and **3e** reveals no more than 6−8 hydrogen bonds between headgroups. Despite the modification of the intermolecular network, the large-scale solid-state structures of **3d** and **3e** are very similar to those observed for bolaforms bearing carbohydrate headgroups. The hydrogen-bonding network established by headgroup stereochemistry affords a pleated sheet structure in the solid state for glucal derivative **3d** (Figure 6A) and a parallel plane orientation for **3e** (Figure 6C), analogous to similar compounds bearing carbohydrate headgroups of identical stereochemistry at C-4 and C-5 (Figure 6B,D).[7,24]

Moreover, this similarity between solid state structures even after loss of a significant portion of the hydrogen bonding network suggests that a relatively low number of intermolecular interactions may be necessary to induce the observed ordering. Interestingly, a diastereomeric mixture of **3d** does not appear to affect the solid-state structure as the α,α (major) and α,β (minor) diastereomers cleanly cocrystallize. Our results are also consistent with the hypothesis that headgroup stereochemistry,

(21) Shimizu, T. *Macromol. Rapid Commun.* **2002**, *23*, 311.
(22) Nakashima, N.; Asakuma, S.; Kunitake, T. *J. Am. Chem. Soc.* **1985**, *107*, 509.
(23) The details of the X-ray crystal study and CIF files for structures **3d** and **3e** have been reported separately: Tice, N.; Parkin, S.; Bozell, J. *J. Carbohydr. Res* **2008**, *343*, 374.
(24) Masuda, M.; Shimizu, T. *Chem. Commun.* **1996**, 1057.

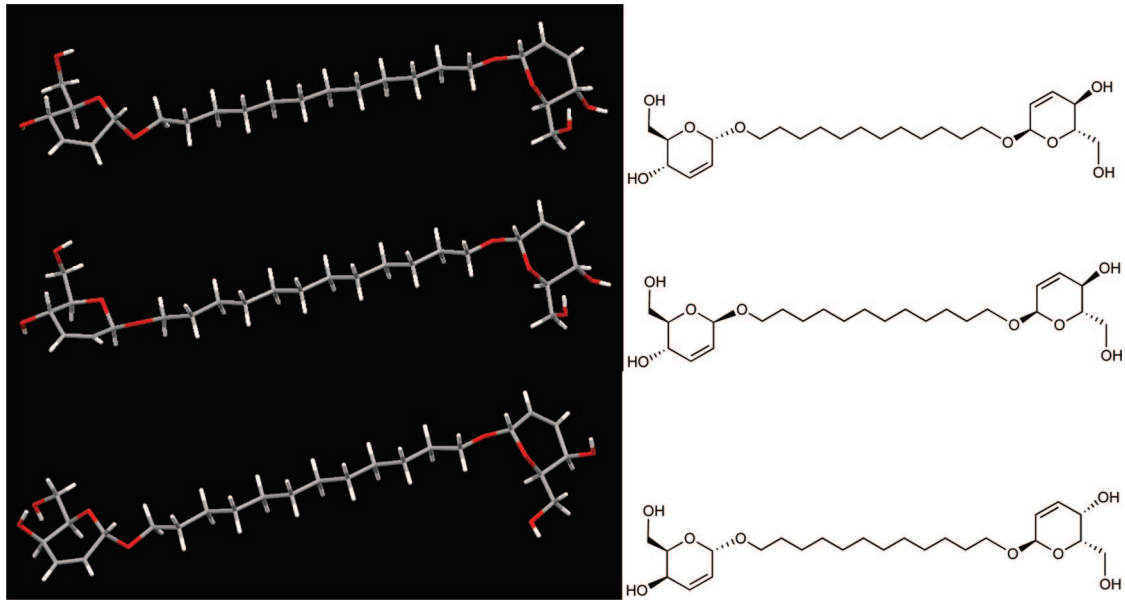

FIGURE 5. X-ray crystal structures of compounds **3d** (major and minor diastereomers) and **3e**.

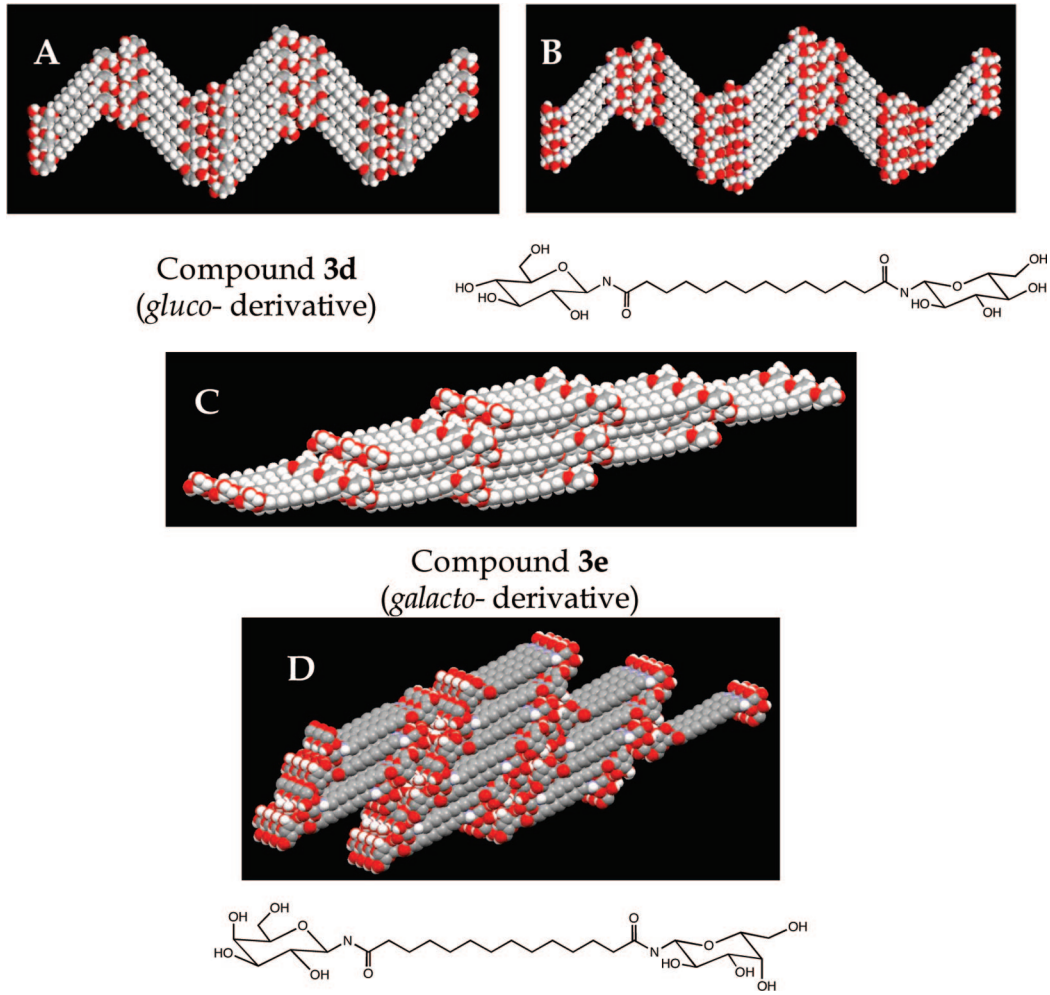

FIGURE 6. Comparative X-ray structures of glycal bolaforms **3d** and **3e** with similar carbohydrate bolaforms.

which establishes the hydrogen bonding network, has the greatest influence on controlling the structure of the final polymolecular arrays.

The correlations between the processes in the solid state and self-assembly in solution remain less clear. Control of bolaform self-assembly is a delicate balance between headgroup shape, length of the chain linking the headgroups, and the hydrophobic and hydrophilic properties of a given molecule.[25] Subtle changes in these properties can result in modification of the observed macromolecular structure. The reduced number of hydrogen-

bonding opportunities in **3d** may result in more transient nanostructures in solution. For those compounds that form stable nanostructures (e.g., **3b** or **3c**), we anticipate that the hydrogen-bonding network is similar to that observed in the solid state. It is also reasonable that **3d** forms an analogous network. Similar retention of structure has been observed for related carbohydrate-based bolaforms upon comparison of cast films with aqueous dispersions.[26] However, other intermolecular forces in **3d** disrupt and overwhelm hydrogen bonding, causing transition to larger aggregates before establishment of an ordered hydrogen bond network. The results of the solution- and solid-state studies indicate that multiple hydrogen bonds in solution are important to formation of stable, discrete nanostructures but that only a few key intermolecular interactions between bolaform headgroups are necessary to determine the structure in the solid state. The synthetic flexibility of glycal-based bolaforms will improve our ability to study these effects. Current efforts are examining enhancement of the hydrogen bond network through incorporation of disaccharide headgroups using the methods shown in Scheme 1. Additional efforts to improve the solubility of these molecules, and better understand the nature and control of the forces responsible for self-assembly are also underway.

Experimental Section

Materials and Methods. THF was distilled from Na/benzophenone ketyl prior to use. Other solvents were reagent grade and used without further purification. All other materials were commercially available and used as received except triacetylgalactal[10] and diacetylxylal,[11] which were prepared by literature methods.

General Procedure for Ferrier Addition of Diols to Glycals. The acetylated glycal and diol (0.5 mmol/mmol glycal; 1 equiv) were dissolved in freshly distilled THF (5 mL of THF/mmol of glycal) and degassed. Catalytic I_2 (3−5 mol % based on glycal) was added as a solid and the solution stirred at room temperature until TLC (petroleum ether/EtOAc mixtures) or HPLC indicated that the reaction was complete. The solution was diluted with a 2× excess of Et_2O and washed twice with 10% aq $Na_2S_2O_3$ (approximately 1 mL/mmol of glycal per wash) and twice with saturated $NaHCO_3$ (approximately 1 mL/mmol of glycal per wash). The organic layer was separated and dried over $MgSO_4$. The solvent was removed on the rotary evaporator and the residue purified by column chromatography on Si gel (hexanes/ether mixtures) to give the acetylated bolaform. In general, acetates were used immediately for the preparation of the corresponding hydroxylated bolaforms. However, typical spectral data are reported below.

1,12-Bis(4,6-di-*O*-acetyl-2,3-dideoxy-α-D-*erythro*-hex-2-enopyranosyloxy)octane (2b): colorless oil, 90%; ^{1}H NMR ($CDCl_3$) 1.26−1.53 (m, 12H), 2.01 (s, 6H), 3.42 (dt, *J*=9.1, 6.6 Hz, 2H), 3.69 (dt, J = 9.5, 6.7 Hz, 2H), 3.97−4.21 (m, 6H), 4.95 (br s), 5.23 (m, 2H), 5.78 (m, 4H); ^{13}C ($CDCl_3$) 20.7, 20.8, 26.1, 29.2, 29.6, 62.9, 65.1, 66.7, 68.8, 94.2, 127.8, 128.9, 170.1, 170.6; IR (neat) 2933, 2859, 1739, 1370, 1223, 1185, 1104, 1032, 981; MS ($C_{28}H_{42}O_{12}$) exact mass ($M + O_2^-$) calcd 602.2575, found 602.2541.

1,12-Bis(4,6-di-*O*-acetyl-2,3-dideoxy-α-D-*erythro*-hex-2-enopyranosyloxy)decane (2c): colorless oil, 81%; ^{1}H NMR ($CDCl_3$) 1.23−1.55 (m, 16H), 2.02 (s, 3H), 2.04 (s, 3H), 3.43 (dt, J = 9.0, 6.3 Hz, 2H), 3.70 (dt, J = 9.5, 6.7 Hz, 2H), 4.01−4.22 (m, 6H), 4.96 (br s, 2H), 5.26 (m, 2H), 5.80 (m, 4H); ^{13}C ($CDCl_3$) 20.7, 20.8, 26.1, 29.3, 29.4, 29.6, 62.9, 65.2, 66.7, 68.8, 94.3, 127.8, 128.9, 170.1, 170.6; IR (neat) 2929, 2856, 1740, 1370, 1223, 1185, 1104, 1032; MS ($C_{30}H_{46}O_{14}$) exact mass ($M + O_2^-$) calcd 630.2888, found 630.2904.

1,12-Bis(4,6-di-*O*-acetyl-2,3-dideoxy-α-D-*erythro*-hex-2-enopyranosyloxy)dodecane (2d): colorless oil, 90%; ^{1}H NMR ($CDCl_3$) 1.12−1.58 (m, 20H), 1.98 (s, 3H), 1.99 (s, 3H), 3.39 (dt, J = 9.6, 6.5 Hz, 2H), 3.66 (dt, J = 9.5, 6.7 Hz, 2H), 3.97−4.18 (m, 6H), 4.92 (br s, 2H), 5.21 (m, 2H), 5.75 (m, 4H); ^{13}C NMR ($CDCl_3$) 20.6, 20.8, 26.1, 29.2, 29.4, 29.5, 62.8, 65.1, 66.7, 68.8, 94.2, 127.8, 128.8, 170.0, 170.5; MS ($C_{32}H_{50}O_{12}$) exact mass ($M - H^+$) calcd 625.3224, found 625.3200.

1,12-Bis(4,6-di-*O*-acetyl-2,3-dideoxy-α-D-*threo*-hex-2-enopyranosyloxy)dodecane (2e): colorless oil, 20%; ^{1}H NMR ($CDCl_3$) 1.16−1.60 (m, 20H), 2.03 (s, 3H), 2.04 (s, 3H), 3.44 (m, 2H), 3.72 (m, 2H), 4.17 (m, 4H), 4.31 (ddd, $J_{5,6}$ = 7.6, 5.2 Hz, $J_{4,5}$ = 2.5 Hz), 4.98 (dd, H4, $J_{3,4}$ = 5.1, $J_{4,5}$ = 2.5 Hz, 2H), 5.01 (d, $J_{1,2}$ = 2.8 Hz, 2H), 5.98 (dd, 2H, $J_{2,3}$ = 10.0 Hz, $J_{1,2}$ = 2.9 Hz), 6.05 (dd, $J_{2,3}$ = 10.4 Hz, $J_{3,4}$ = 4.8 Hz, 2H); ^{13}C NMR ($CDCl_3$) 20.7, 20.8, 26.2, 29.4, 29.5, 29.6, 62.8, 66.6, 68.5, 93.7, 125.0, 130.7, 170.3, 170.5; IR (neat): 2926, 2855, 1737, 1369, 1224, 1189, 1104, 1044, 1013; MS ($C_{32}H_{50}O_{12}$) exact mass ($M + O_2^-$) calcd 658.3201, found 658.3207.

1-(4-*O*-Acetyl-2,3-dideoxy-α-D-*glycero*-pent-2-enopyranosyloxy)-12-(4-*O*-acetyl-2,3-dideoxy-β-D-*glycero*-pent-2-enopyranosyloxy)-dodecane (2f, α,β-isomer). white powder, 25%; ^{1}H NMR ($CDCl_3$) 1.14−1.62 (m, 20H), 2.01 (s, 3H), 2.04 (s, 3H), 3.42 (dt, 2H, J = 9.5, 6.6 Hz), 3.67−3.84 (m, 6H), 4.11 (dd, 1H, $J_{5,5}$ = 13.0 Hz, $J_{4,5}$ = 2.8 Hz), 4.88 (m, 2H), 4.94 (d, $J_{1,2}$ = 2.0 Hz, 1H), 5.22 (m, 1H), 5.82 (ddd, 1H, $J_{2,3}$ = 10.3 Hz, $J_{3,4}$ = 3.6 Hz, $J_{1,2}$ = 1.7 Hz), 5.89 (br d, 1H, $J_{2,3}$ = 10.4 Hz), 6.0 (m, 2H); ^{13}C NMR ($CDCl_3$) 21.0, 21.1, 26.1, 29.4, 29.5, 29.7, 60.1, 61.1, 63.3, 65.0, 68.6, 68.8, 92.9, 94.2, 124.8, 128.6, 129.3 131.0, 170.5, 170.6; IR (neat) 2918, 2886, 2846, 1727, 1467, 1447, 1367, 1236, 1196, 1047; MS ($C_{26}H_{42}O_{10}$) exact mass ($M + O_2^-$) calcd 514.2778, found 514.2756; mp 72−74 °C.

1,12-Bis(4-*O*-acetyl-2,3-dideoxy-β-D-*glycero*-pent-2-enopyranosyloxy)dodecane (2f, β,β-isomer): white powder, 29%; ^{1}H NMR ($CDCl_3$) 1.17−1.61 (m, 20H), 2.06 (s, 3H), 3.44 (dt, 2H, J = 9.5, 6.6 Hz), 3.73 (dt, 2H, J = 9.5, 6.8 Hz), 3.79 (d, $J_{5,5}$ = 13 Hz), 4.12 (dd, $J_{5,5}$ = 13 Hz, $J_{4,5}$ = 2.8 Hz), 4.91 (ddd, $J_{3,4}$ = 3.98 Hz, $J_{4,5}$ = 2.91 Hz, $J_{2,4}$ = 0.91 Hz, 2H), 4.96 (d, $J_{1,2}$ = 2.04 Hz, 2H), 6.01 (m, 4H); ^{13}C NMR ($CDCl_3$) 21.1, 26.1, 29.3, 29.5, 29.7, 61.1, 63.3, 68.6, 92.9, 124.8, 131.0, 170.6; IR (neat) 2918, 2850, 1728, 1373, 1252, 1108, 1043, 1006, 954; MS ($C_{22}H_{38}O_8$) exact mass ($M + O_2^-$) calcd 514.2778, found 514.2782; mp 76−78 °C.

General Procedure for Zemplén Deprotection of Bolaform Acetates. The bolaform acetate was dissolved in MeOH (approximately 10 mL/mmol of bolaform) and was treated with a catalytic amount (5 mol %) of NaOMe (as a 0.5 M solution in MeOH). The solution was stirred until TLC (petroleum ether/EtOAc mixtures) or HPLC indicated that the reaction was complete. The solvent was removed on the rotary evaporator and the residue taken up in the minimum amount of hot EtOH. Cooling of the solution generally gave the corresponding bolaform as a white solid.

1,8-Bis(2,3-dideoxy-α-D-*erythro*-hex-2-enopyranosyloxy)octane (3b): white powder, 69%; ^{1}H NMR (CD_3OD) 1.35−1.62 (m, 12H), 3.48 (m, 2H), 3.61−3.91 (m, 8H), 4.2 (m, 2H), 4.96 (m, 2H), 5.72 (ddd, $J_{2,3}$ = 10.16 Hz, J = 2.69 Hz, $J_{1,2}$ = 2.07 Hz, 2H), 5.93 (m, $J_{2,3}$ = 10.2 Hz, $J_{3,4}$ = 1.4 Hz, 2H); ^{13}C NMR (CD_3OD) 27.3, 30.5, 30.8, 62.7, 64.2, 69.4, 73.6, 95.4, 127.3, 134.6; IR (neat) 3316, 2020, 2852, 1434, 1390, 1326, 1262, 1189, 1104, 1044, 978; MS ($C_{20}H_{34}O_8$) exact mass ($M - H^+$) calcd 401.2175, found 401.2186; mp 105.5−106.5 °C. Anal. Calcd: C, 59.68; H, 8.51; O, 31.80. Found: C, 59.52; H, 8.52; O, 31.96.

1,10-Bis(2,3-dideoxy-α-D-*erythro*-hex-2-enopyranosyloxy)decane (3c): white powder, 83%; ^{1}H NMR (CD_3OD) 1.32−1.61 (m, 16H), 3.48 (m, 2H), 3.59−3.91 (m, 8H, OCH_2), 4.02 (m, 2H), 4.96 (m, 2H), 5.72 (ddd, $J_{2,3}$ = 10.2 Hz, $J_{1,2}$ = 2.6 Hz), 5.91 (m, $J_{2,3}$ = 10.1 Hz); ^{13}C NMR (CD_3OD) 27.4, 30.6, 30.7, 30.9, 62.7, 64.2, 69.5, 73.6, 95.5, 127.3, 134.6; IR (neat) 3295, 2920, 2853, 1467,

(25) (a) Benvegnu, T.; Lecollinet, G.; Guilbot, J.; Roussel, M.; Brard, M.; Plusquellec, D. *Polym. Int.* **2003**, *52*, 500. (b) Claessens, C. G.; Stoddart, J. F. *J. Phys. Org. Chem.* **1997**, *10*, 254.

(26) Kameta, N.; Masuda, M.; Minamikawa, H.; Shimizu, T. *Langmuir* **2007**, *23*, 4634.

1388, 1284, 1180, 1054, 999; MS ($C_{22}H_{38}O_8$) exact mass (M − H^+) calcd 429.2488, found 429.2463; mp 109.5−110.5 °C. Anal. Calcd: C, 61.37; H, 8.90; O, 29.73. Found: C, 61.03; H, 8.83; O, 30.14.

1,12-Bis(2,3-dideoxy-α-D-*erythro*-hex-2-enopyranosyloxy)dodecane (3d)[27]: white powder, 74%; ^{1}H NMR (CD_3OD) 1.26−1.66 (m, 20H), 3.50 (dt, 2H, J = 9.5, 6.4 Hz), 3.60−3.89 (m, 8H), 4.03 (m, 2H), 4.96 (br s, 2H), 5.71 (ddd, 2H, $J_{2,3}$ = 10.1 Hz, $J_{3,4}$ = 2.7 Hz), 5.90 (m, 2H, $J_{2,3}$ = 10.1 Hz); ^{13}C NMR (CD_3OD) 27.3, 30.5, 30.7, 30.9, 62.7, 64.2, 69.5, 73.6, 95.5, 127.3, 134.6; IR (neat) 3291, 2918, 2852, 1470, 1386, 1310, 1183, 1149, 1057, 996, 964; MS ($C_{24}H_{42}O_8$) exact mass (M − H^+) calcd 457.2801, found 457.2810; mp 115−116 °C. Anal. Calcd: C, 62.14; H, 9.07; O, 28.79. Found: C, 62.32; H, 9.13; O, 28.55.

1,12-Bis(2,3-dideoxy-α-D-*threo*-hex-2-enopyranosyloxy)dodecane (3e): white powder, 80%; ^{1}H NMR (CD_3OD) 1.24−1.65 (m, 20H), 3.46 (dt, J = 9.6, 6.5 Hz, 2H), 3.67−3.88 (m, 8H), 3.97 (ddd, $J_{4,5}$ = 7.43 Hz, $J_{3,4}$ = 5.30 Hz, J = 2.35 Hz, 2H), 4.99 (d, 2H, $J_{1,2}$ = 3.0 Hz), 5.88 (dd, 1H, $J_{2,3}$ = 10.0 Hz, $J_{1,2}$ = 3.1 Hz), 6.07 (ddd, $J_{2,3}$ = 10.0 Hz, $J_{3,4}$ = 5.5 Hz, J = 0.9 Hz); ^{13}C NMR (CD_3OD) 27.4, 30.6, 30.8, 30.9, 62.2, 62.8, 69.2, 72.8, 95.5, 129.5, 130.3; IR (neat) 3295, 2934, 2916, 2815, 1471, 1385, 1246, 1185, 1098, 1047, 996; MS ($C_{24}H_{42}O_8$) exact mass (M − H^+) calcd 457.2801, found 457.2807; mp 118.5−119.5 °C. Anal. Calcd: C, 62.14; H, 9.07; O, 28.79. Found: C, 62.40; H, 9.19; O, 28.41.

1-(2,3-Dideoxy-α-D-*glycero*-pent-2-enopyranosyloxy)-12-(2,3-dideoxy-β-D-*glycero*-pent-2-enopyranosyloxy)dodecane (3f, α,β-isomer): white powder, 37%; ^{1}H NMR (CD_3OD) 1.25 (m, 16H), 1.52 (m, 4H), 3.36−3.79 (m, 8H), 3.9 (m, 1H), 4.1 (m, 1H), 4.84 (br d, J = 2 Hz), 5.6−5.8 (m, 2H), 5.85−6.0 (m, 2H); ^{13}C NMR (CD_3OD) 27.3, 30.5, 30.7, 30.8, 30.9, 62.1, 63.7, 65.5, 69.2, 69.5, 94.8, 95.4, 127.8, 129.5, 129.9, 134.6; IR (neat) 3439, 3362, 2918, 2852, 1484, 1390, 1320, 1094, 1043, 1000; MS ($C_{22}H_{38}O_8$) exact mass (M + O_2^-) calcd 430.2567, found 430.2548; mp 95−97 °C.

1,12-Bis(2,3-dideoxy-β-D-*glycero*-pent-2-enopyranosyloxy)dodecane (3f, β,β-isomer): white powder, 80%; ^{1}H NMR (CD_3OD) 1.30 (m, 16H), 1.57 (m, 4H), 3.46 (dt, 2H, J = 9.6, 6.5 Hz), 3.66 (dt, 2H, $J_{5,5}$ = 12.15 Hz, $J_{4,5}$ = 1.49 Hz), 3.73 (dt, 2H, J = 9.6, 6.7, Hz), 3.8 (m, 2H), 4.03 (dd, 2H, J = 2.91 Hz), 4.92 (dd, 2H, $J_{1,2}$ = 2.92 Hz, J = 0.98 Hz), 5.84 (ddd, 2H, $J_{2,3}$ = 10.10 Hz, $J_{1,2}$ = 3.00 Hz, J = 0.72 Hz), 6.02 (dddd, 2H, $J_{2,3}$ = 10.07 Hz, $J_{3,4}$ = 5.03 Hz, J = 1.24 Hz); ^{13}C NMR (CD_3OD) 27.3, 30.5, 30.7, 30.8, 62.1, 65.5, 69.2, 94.8, 129.5, 129.9; IR (neat) 3379, 2920, 2851, 1449, 1434, 1327, 1262, 1190, 1099, 1042; mp 88−90 °C. Anal. Calcd: C, 65.60; H, 9.44; O, 24.97. Found: C, 65.47; H, 9.52; O, 25.01.

1-(2,3-Dideoxy-α-D-*erythro*-hex-2-enopyranosyloxy)-12-(2,3-dihydro-β-D-*erythro*-hexopyranosyloxy)dodecane (5): white powder; ^{1}H NMR (CD_3OD) 1.25−1.86 (m, 24H), 3.33−3.57 (m, 4H, OCH_2), 3.61−3.87 (m, 7H), 4.01 (m, 1H), 4.75 (br s, 1H), 4.95 (br s, 1H, 5.72 (ddd, 1H, $J_{2,3}$ = 10.2 Hz, $J_{1,2}$ = 2.7 Hz), 5.90 (m, 1H, $J_{2,3}$ = 10.2 Hz); ^{13}C NMR (CD_3OD) 27.4, 27.5, 28.3, 30.5, 30.6, 30.7, 30.8, 30.9, 62.8, 631. 64.2, 67.1, 68.0, 69.5, 73.6, 75.3, 95.5, 97.3, 127.3, 134.7; IR (neat) 3297, 2934, 2918, 2815, 1471, 1386, 1284, 1182, 1127, 1052, 998, 996; MS ($C_{24}H_{44}O_8$) exact mass (M − H^+) calcd 459.2958, found 459.2933; mp 102−104 °C. Anal. Calcd: C, 61.86; H, 9.48; O, 28.66. Found: C, 62.10; H, 9.56; O, 28.34.

6-Dodecyloxy-2-hydroxymethyl-3,6-dihydro-2*H*-pyran-3-ol (6). To a dry, three-necked round-bottom flask were added tri-*O*-acetyl-D-glucal (1.254 g, 4.61 mmol) and 1-dodecanol (0.858 g, 4.61 mmol). The flask was degassed. Dry solvent (approximately 4 mL/mmol triacetylglucal) was added to the flask via syringe under argon, and the mixture was stirred for about 15 min. To the resulting solution was quickly added iodine (0.230 mmol, 0.05 equiv), and the reaction was stirred at room temperature for 6 h. The reaction mixture was poured in a separatory funnel and diluted with 25 mL of ether. The solution was washed with 2 × 15 mL of 10% $Na_2S_2O_3$. The organic layer was dried over anhydrous $MgSO_4$ and filtered through Celite in a sintered funnel. Evaporation of the solvent gave a crude oil that was purified by silica gel column chromatography using 8:1 hexane/ethyl acetate as eluent to give the intermediate acetate (82%): ^{1}H NMR ($CDCl_3$) 0.81−0.84 (t, 3H, J = 12 Hz), 1.21 (br s, 20 H), 1.52−1.55 (m, 1H), 2.062 (s, 6H), 3.39−3.46 (m, 1H), 3.71−3.74 (m, 1H), 4.05−4.22 (m, 2H), 4.99 (br s, 1H), 5.27 (d, 1H, J = 12 Hz), 5.80−5.83 (m, 2H). The acetate (0.900 g, 2.26 mmol) was placed in a round-bottom flask. Anhydrous methanol (33 mL) was added and the solution stirred for 15 min. Sodium methoxide in methanol (0.5 M, 0.1 equiv) was added, and the solution was stirred for 5 h. Removal of solvent from the reaction mixture under reduced pressure gave **6** as a white powder (0.52 g, 73%). The product was purified by recrystallization from hot hexane/ethyl acetate to give a white solid (mp 63 °C): ^{1}H NMR (CD_3OD) 1.01 (t, 3H, J = 6 Hz), 1.40 (br m, 20 H), 1.66−1.72 (dd, 1H, J = 6 Hz), 3.42−3.50 (m, 1H), 3.56−3.58 (m, 1H), 3.73−3.76 (m, 1H), 3.79−3.82 (m, 1H), 4.12−4.14 (d, 1H, J = 8 Hz), 5.06 (br d, 1H), 5.81−5.83 (m, 1H), 5.99−6.02 (m, 1H); ^{13}C NMR (CD_3OD) δ 11.5, 20.8, 24.4, 27.5, 27.6, 27.8, 27.9, 30.1, 59.8, 61.3, 66.6, 70.7, 92.5, 124.4, 131.7; IR (neat) 3310; MS (EI, *m*/*z*) 313 (M^+), 298, 297, 295, 283, 257, 254, 241, 239, 143, 129; MS ($C_{18}H_{34}O_4$) exact mass (M − H^+) calcd 313.2379, found 313.2358. The α/β ratio was determined by integration of the ring H4 peaks at 5.27 ppm in the NMR spectrum.

$TiCl_4$-Catalyzed Reaction of Triacetylglucal and 1-Dodecanol in THF or CH_2Cl_2. To a dry, three-necked round-bottom flask were added tri-*O*-acetyl-D-glucal **3** (1.118 g, 4.11 mmol) and 1-dodecanol **4** (0.765 g, 4.11 mmol). The flask was degassed and left under argon for 10 min. Twenty milliliters of freshly distilled THF or CH_2Cl_2 was added to the flask via syringe under argon, and the mixture was stirred for 15 min. The resulting solution was cooled to −78 °C (CO_2/*i*-PrOH). To the resulting solution was quickly added $TiCl_4$ (6.2 mL, 1.5 equiv) and the mixture stirred for 6 h at −78 °C. The reaction mixture was poured into a separatory funnel, diluted with 25 mL of ether, and washed with 2 × 15 mL of saturated $NaHCO_3$ solution. The organic layer was dried over anhydrous $MgSO_4$ and filtered through Celite in a sintered funnel. Evaporation of solvent gave the intermediate acetate that was purified by column chromatography using 8:1 hexanes/ethyl acetate to yield a colorless oil (71% in THF, or 0.77 g, 46% in CH_2Cl_2).

Bolaform Dispersion and Self-Assembly: Bolaform 3b. Compound **3b** (10.9 mg) was mixed with 500 μL of water at room temperature. It was heated gently with a heat gun to give a homogeneous and slightly opaque solution that was not clarified by filtering. Addition of a further 500 μL of H_2O did not induce any apparent precipitation. The sample remained homogeneous for several weeks.

Bolaform Dispersion and Self-Assembly: Bolaform 3c. Compound **3c** (11.2 mg) was mixed with 500 μL of water at room temperature. Upon heating with a heat gun, the material dissolved to give a milky, opaque solution. Upon cooling to room temperature, the bolaform began to precipitate. Addition of 250 μL of 1,4-dioxane caused much of the precipitated solid to dissolve. Brief heating gave a clear, colorless solution that remained homogeneous for weeks. Addition of 250 μL of water to the clear solution induced some precipitation after about 30 min.

Bolaform Dispersion and Self-Assembly: Bolaform 3d. Compound **3d** (10.6 mg) was mixed with 500 μL of water at room temperature. Upon heating with a heat gun, the material dissolves to give a clear, colorless solution. Upon removal of the heat, precipitation begins almost immediately and is complete within 5 min. Addition of 500 μL of 1,4-dioxane and heating affords a clear, colorless solution that retains its solubility for a number of days.

(27) Synthesis of this compound in 45% yield has been reported from the Ferrier reaction of triacetylglucal and 1,12-dodecanediol in the presence of BF_3 etherate. However, the NMR reported exhibits some differences in comparison to our spectra, and a calculated molecular weight of 636 is reported, while the actual molecular weight of this compound is 626. Moreover, when we repeated the literature method, spectra matching ours were obtained. See: Wieczorek, E.; Thiem, J. *J. Carbohydr. Chem* **1998**, *17*, 785.

Addition of 250 μL of water to the clear solution induces some precipitation after about 30 min.

General Procedure for Transmission Electron Microscopy Experiments. Transmission electron microscopy was carried out at 80 KeV. The samples were prepared by placing a drop of the bolaform solution on a hydrophobic surface and gently dragging a 300 mesh carbon coated Cu grid across the drop. The excess solution was blotted with filter paper and the sample stained with 1% aqueous uranyl acetate and allowed to dry briefly in air before imaging.

Acknowledgment. This work was supported by the U.S. Department of Agriculture Wood Utilization Research Program and the University of Tennessee Institute of Agriculture. Initial synthetic work by Mr. Joseph Bullock as part of a U.S. Department of Energy summer internship program is gratefully acknowledged. X-ray analyses were carried out by Dr. Sean Parkin of the University of Kentucky. TEM measurements at the University of Tennessee were carried out by Dr. John Dunlap.

Supporting Information Available: NMR spectra for compounds **2b**−**f**, **3b**−**f**, **5**, and **6** are presented. Full X-ray data for the α,α and α,β isomers of compound **3f** are presented. This material is available free of charge via the Internet at http://pubs.acs.org.

JO801341G